Available online at www.sciencedirect.com

ScienceDirect

Ceramics International 37 (2011) 1959–1965

CERAMICS INTERNATIONAL

www.elsevier.com/locate/ceramint

Effects of $NaTaO_3$ additions on structure and electrical properties of $K_{0.5}Na_{0.5}NbO_3$–$Bi_{0.5}Na_{0.5}TiO_3$–$LiSbO_3$ piezoelectric ceramics

Yixiong Liu [a,b], Yanqiu Huang [a,b,*], Huilin Li [a,b], Haiwei Du [a,b], Hongping Tang [a,b], Guoxi Zhang [a,b]

[a] *Faculty of Materials Science and Chemical Engineering, China University of Geosciences, No. 388, Lumo Road, Wuhan 430074, PR China*
[b] *Engineering Research Center of Nano-Geomaterials of Ministry of Education (China University of Geosciences), Wuhan 430074, PR China*

Received 13 January 2011; accepted 17 February 2011
Available online 23 February 2011

Abstract

The $(1-x)(0.9405K_{0.5}Na_{0.5}NbO_3$–$0.0095Bi_{0.5}Na_{0.5}TiO_3$–$0.05LiSbO_3)$–$xNaTaO_3$ lead-free piezoelectric ceramics were fabricated by conventional ceramic technique. The structure, dielectric, ferroelectric and piezoelectric properties of the ceramics were investigated. The X-ray diffraction (XRD) analysis revealed that the ceramics sintered in air at 1060–1140 °C for 3–4 h formed single phase pervoskite solid solutions with the tetragonal symmetry at room temperature. The microstructure of the ceramics became homogeneous with addition of $NaTaO_3$. The orthorhombic–tetragonal transition temperature (T_{O-T}) shifted to below room temperature with addition of $NaTaO_3$. The dielectric and piezoelectric properties of ceramics were enhanced by addition of $NaTaO_3$. The outstanding electrical properties of piezoelectric coefficient $d_{33} = 249$ pC/N, electromechanical coupling factors, $k_p = 0.442$ and $k_t = 0.426$, relative permittivity, $\varepsilon_{33}^T/\varepsilon_0 = 1604$ and loss tangent, $\tan\delta = 0.023$ were obtained at $x = 0.06$. The related physical mechanisms for the enhancement of dielectric and piezoelectric properties were discussed.

Keywords: C. Dielectric properties; C. Piezoelectric properties; D. Niobates

1. Introduction

Lead-free piezoelectric materials have generated enormous research interest since the end of the 1990s because of an increased environmental awareness [1]. Among different lead-free materials, the (K,Na)NbO_3-based ceramics have attracted significant attention due to their outstanding dielectric and electromechanical properties and high Curie temperature (T_C) [2,3]. However, compared with the commercial Pb(Zr,Ti)O_3-based ceramics, the sintering behavior, piezoelectric performance and temperature stability of the (K,Na)NbO_3-based ceramics need to be further improved. In recent years, numerous studies have been devoted to (K,Na)NbO_3-based ceramics with focus on obtaining dense ceramics with good performance by optimizing sintering processes and compositional modifications [4]. Various ABO_3-type compounds such as $LiSbO_3$, $LiNbO_3$, $LiTaO_3$, $SrTiO_3$, $CaTiO_3$, $(Na_{0.5}Bi_{0.5})TiO_3$, $BiScO_3$, $BiFeO_3$ and $NaSbO_3$ have been added into (K,Na)NbO_3 to form (K,Na)NbO_3-based solid solution ceramics [5–13]. It is reported that the (K,Na)NbO_3-based solid solution ceramics with an orthorhombic–tetragonal polymorphic phase transition (PPT) near room temperature exhibit excellent piezoelectric properties owing to the increased amount of spontaneous polarization vectors [14,15]. Nevertheless, it should be noted that those (K,Na)NbO_3-based ceramics possess low temperature stability for the PPT near or at room temperature, which limits their practical applications [16,17]. Therefore, it is very important to promote the temperature stability of the electrical properties of (K,Na)NbO_3-based ceramics from the viewpoint of application. As expected, the temperature stability of (K,Na)NbO_3-based ceramics can be improved by shifting the PPT below room temperature or choosing a composition on the tetragonal side [14,18,19]. In the case of perovskite ferroelectrics, it should be emphasized that the piezoelectric coefficient d is not only affected by the extrinsic contributions which mainly originate from the domain wall or phase boundary motions, but also affected by the intrinsic piezoelectric responses. It is well known that the intrinsic piezoelectric coefficient d_{33} in the tetragonal crystals is proportional to the relative permittivity ε_{33}

---

* Corresponding author. Tel.: +86 27 87483374.
E-mail address: y.q.huang@163.com (Y. Huang).

0272-8842/$36.00 © 2011 Elsevier Ltd and Techna Group S.r.l. All rights reserved.
doi:10.1016/j.ceramint.2011.02.008

and remnant polarization P_r [20]. Therefore, the improvement of piezoelectric performance can be implemented by designing a composite with large polarization and dielectric permittivity as well as having a PPT below room temperature.

It was found in our previous studies that substitutions of $Bi_{0.5}Na_{0.5}TiO_3$ and $LiSbO_3$ could significantly enhance the dielectric and piezoelectric properties of the (K,Na)NbO_3-based ceramics by forming the orthorhombic–tetragonal polymorphic phase boundary near room temperature [21]. $NaTaO_3$ has the same crystal structure (orthorhombic, space group *Pbnm*) as $CaTiO_3$ and possesses a negative temperature coefficient of permittivity [22]. Previous studies have shown that the addition of $NaTaO_3$ resulted in the decrease of the temperatures of the dielectric anomalies of the $Na(Ta_{1-x}Nb_x)O_3$ ceramics and $(1-x)(Na_{0.5}Bi_{0.5})TiO_3$–$x$NaTaO$_3$ ceramics [23,24]. It is anticipated that the addition $NaTaO_3$ into (K,Na)NbO_3-based ceramics could improve the dielectric and piezoelectric properties of the ceramics by shifting the PPT to low temperature. In this work, $NaTaO_3$ was added into the system of $K_{0.5}Na_{0.5}NbO_3$–$Bi_{0.5}Na_{0.5}TiO_3$–$LiSbO_3$ to form a new kind of solid solution ceramics. The effects of $NaTaO_3$ on the structure and electrical properties of the solid solution ceramics were studied, and the related physical mechanisms were discussed.

2. Experimental details

The ceramics of $(1-x)(0.9405K_{0.5}Na_{0.5}NbO_3$–$0.0095Bi_{0.5}Na_{0.5}TiO_3$–$0.05LiSbO_3)$–$x$NaTaO$_3$ (abbreviated as $(1-x)$KNNBNTLS–xNT, $x = 0$, 0.02, 0.04, 0.06, 0.08, 0.1) were prepared by conventional solid-state reaction technique. Reagent-grade carbonate and oxide powders of K_2CO_3, Na_2CO_3, Li_2CO_3, Bi_2O_3, TiO_2, Nb_2O_5, Sb_2O_3 and Ta_2O_5 were used as starting raw materials. The powders were mixed in stoichiometric proportions and milled in ethanol for 12 h, then dried and calcined at 850 °C for 5 h. The calcined powders were reground and mixed with 7 wt% polyvinyl alcohol (PVA) solution as binder, and then pressed into discs with a diameter of 20 mm. The green discs were finally sintered in air at 1060–1140 °C for 3–4 h. The electrodes were printed on the surfaces of the discs by firing silver paste at 600 °C for 20 min. The specimens were poled in silicone oil at 100 °C for 30 min by applying a dc field of 4–6 kV/mm.

The crystal structure of the sintered samples was determined by X-ray diffraction (XRD) (X′ Pert PRO) with a Cu Kα radiation. The microstructure was observed using a scanning electron microscopy (SEM) (JSM-6700F). The bulk density was measured by the Archimedes method using a Sartorius ED124S 4-digit electronic balance. Dielectric measurements were carried out by a TH2819 precision LCR meter at 10 kHz. The polarization versus electric field (P–E) hysteresis loops of the ceramics were measured using radiant precision ferroelectric measurement system at 10 Hz. The piezoelectric constant d_{33} was measured by a quasistatic piezoelectric constant testing meter (ZJ-3A). The electromechanical coupling factors, k_p, k_t, and the mechanical quality factor Q_m were determined by a resonance–antiresonance method using the Agilent 4294A precision impedance analyzer.

3. Results and discussion

Fig. 1 shows the XRD patterns of the $(1-x)$KNNBNTLS–xNT ceramics with $x = 0$, 0.02, 0.04, 0.06, 0.10. It is found that the samples form single-phase solid solutions with pervoskite

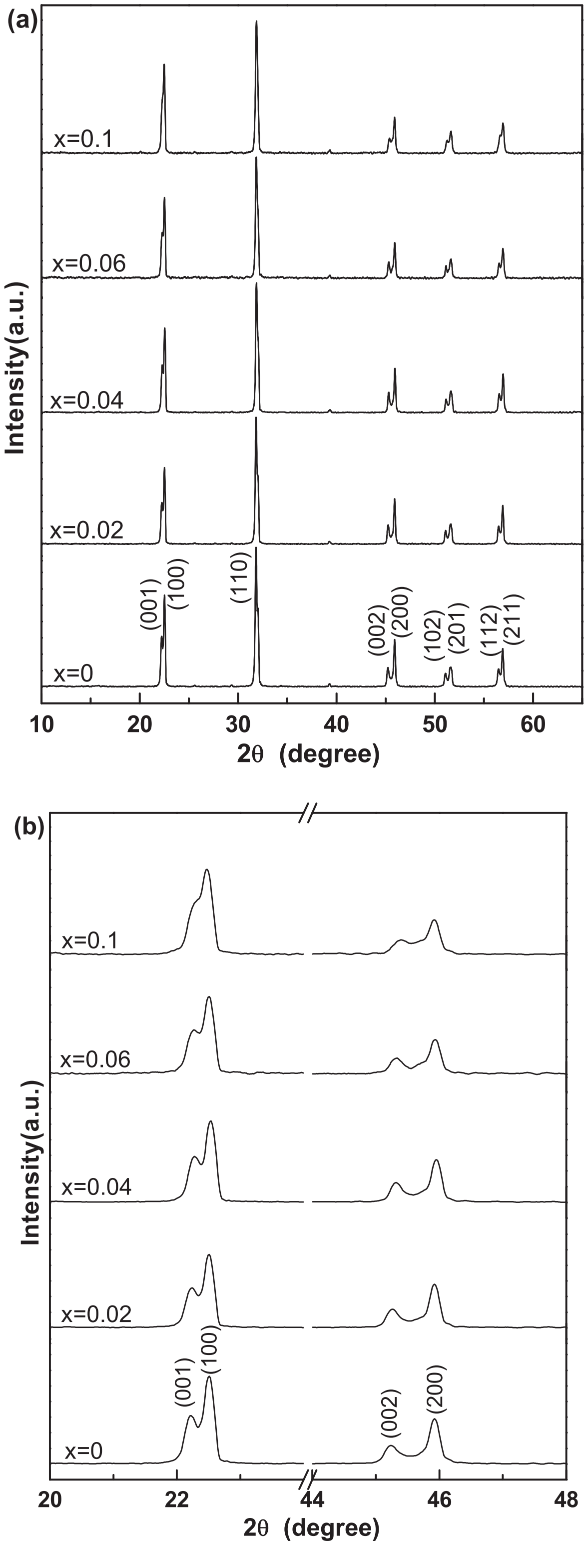

Fig. 1. XRD patterns of the $(1-x)$KNNBNTLS–xNT ceramics (a) wide range and (b) selected portions.

Table 1
Lattice parameters of the $(1-x)$KNNBNTLS–xNT solid solutions with different x.

x	a (Å)	c (Å)	c/a ratio	Volume (Å^3)
0	3.9531	4.0069	1.0136	62.6158
0.02	3.9518	4.0047	1.0134	62.5403
0.04	3.9558	3.9972	1.0105	62.5496
0.06	3.9538	4.0001	1.0117	62.5317
0.10	3.9539	3.9804	1.0067	62.2269

structure, which suggests that $NaTaO_3$ has diffused into the $(K,Na)NbO_3$ lattices. The characteristics of the enlarged XRD patterns (Fig. 1(b)) show that the crystal structure of the ceramics possesses a tetragonal symmetry [18]. Moreover, it can be seen that the diffraction peaks of the ceramics shift to higher angles with increasing x, which indicates that the lattice parameters have a small shrinkage owing to the relatively smaller ionic radius of Na^+ and Ta^{5+} compared to that of K^+ and Nb^{5+} [25,26]. The variations of the lattice parameters of the $(1-x)$KNNBNTLS–xNT solid solutions with the content of NT are summarized in Table 1. It is seen that the lattice parameter c and the unit cell volumes of the solid solutions decrease slightly as x increases whereas the tetragonality c/a of the solid solutions declines with increasing x. These results differ from the $LiTaO_3$-modified $(K,Na)NbO_3$-based ceramics, in which the tetragonality c/a of the solid solutions increases gradually with the increase of $LiTaO_3$ [5,27].

Fig. 2 shows the SEM micrographs of the fracture surfaces of the ceramics with different contents of NT. It is found that all the ceramics have a dense microstructure with little porosity. The shape of the crystal grains changes a little and the microstructure of the ceramics becomes more homogeneous as the addition of NT increases. The grain size of KNNBNTLS ($x = 0$) ceramic is in the range of 0.5–1.5 μm, and that of the ceramic with $x = 0.06$ is about 1–1.5 μm. The bulk density of the $(1-x)$KNNBNTLS–xNT ceramics is shown in Fig. 3. It can be seen that the bulk density increases initially with increasing x, reaching the maximum value of 4.552 g/cm^3 at $x = 0.06$, and then decreases slightly as x increases further. These results suggested that the density of the $(1-x)$KNNBNTLS–xNT ceramics can be enhanced by addition of $NaTaO_3$.

Fig. 4 shows the temperature dependence of the relative permittivity, ε_r, and loss tangent, $\tan\delta$, of the unpoled $(1-x)$KNNBNTLS–xNT ceramics at 10 kHz. As shown in Fig. 4(a), the Curie temperature (T_C) and the temperature of orthorhombic–tetragonal phase transition (T_{O-T}) are observed in the pure KNNBNTLS ceramic. The T_{O-T} of the pure KNNBNTLS ceramic is about 50 °C. This is in good agreement with our XRD result at room temperature, where the pure

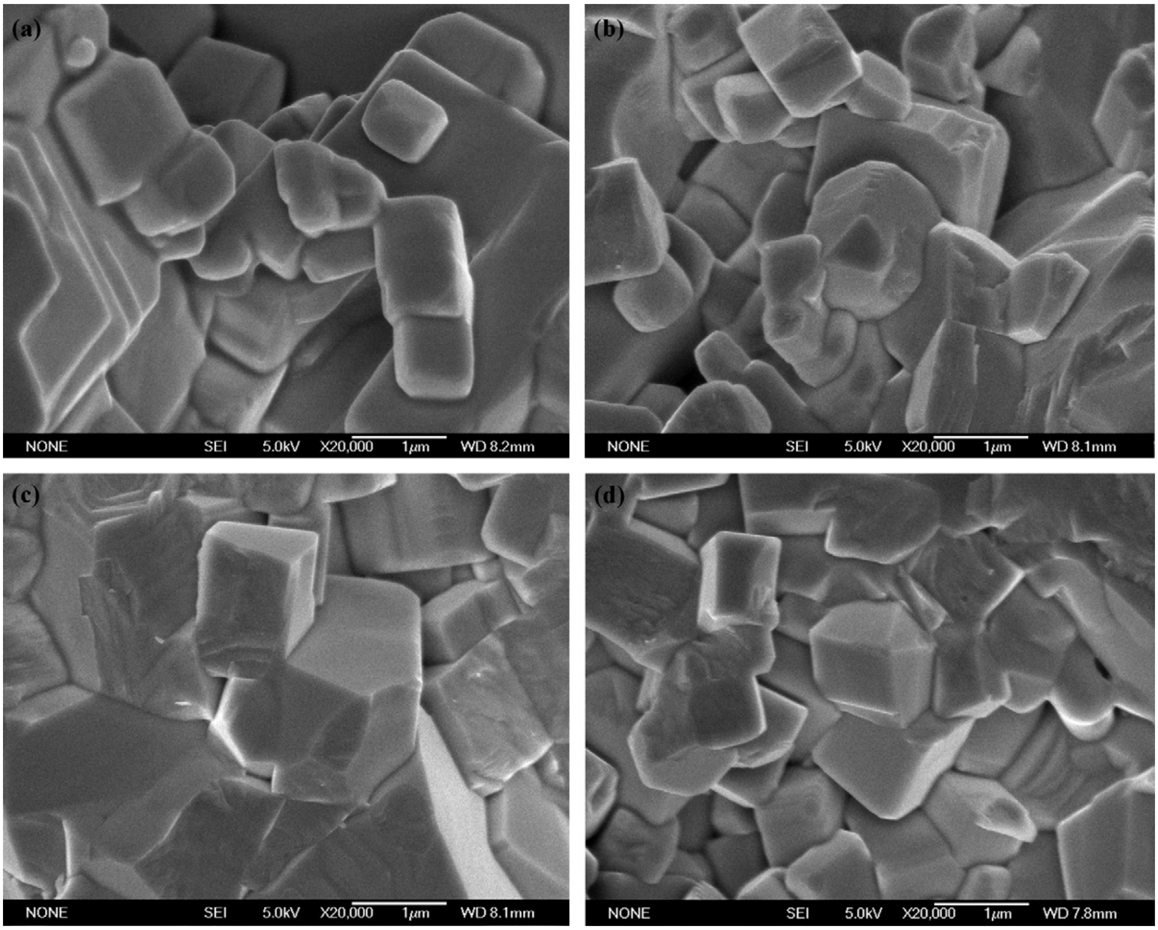

Fig. 2. SEM micrographs of the fracture surfaces of the $(1-x)$KNNBNTLS–xNT ceramics with (a) $x = 0$, (b) $x = 0.02$, (c) $x = 0.06$, and (d) $x = 0.1$.

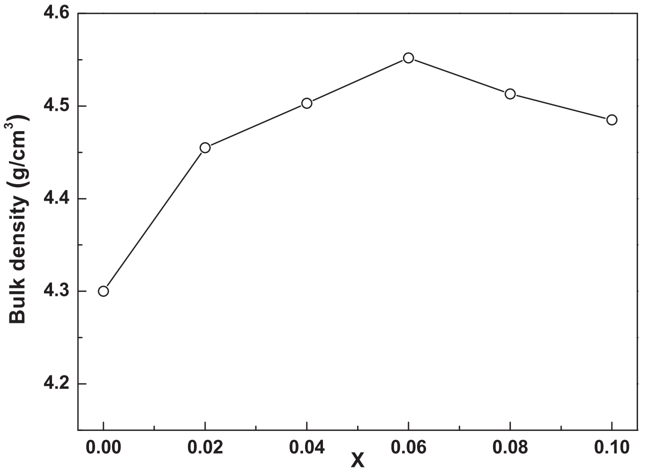

Fig. 3. Bulk density of the (1 − x)KNNBNTLS–xNT ceramics as a function of x.

KNNBNTLS ceramic exhibits a tetragonal symmetry. When $NaTaO_3$ is added, T_C and $T_{O–T}$ shift to lower temperature. The T_C of the (1 − x)KNNBNTLS–xNT ceramics decreases from 356 °C to 268 °C as x increases from 0 to 0.1. According to the results of XRD analysis, the lattice parameters have a small shrinkage and the tetragonality c/a declines with increasing $NaTaO_3$, which could cause the decrease of T_C of the ceramics [27–29]. Meanwhile, it can be clearly seen from the inset of Fig. 4(a) that the peak of the ε_r–T curves near $T_{O–T}$ becomes gradually broadened and then almost disappears above room temperature as x increases, which indicates that the addition of $NaTaO_3$ shifts the $T_{O–T}$ of the (1 − x)KNNBNTLS–xNT ceramics below room temperature. It should be noted that the temperature stability of (K,Na)NbO_3-based ceramics can be improved by shifting the $T_{O–T}$ below room temperature [14,18]. As shown in Fig. 4(b), the (1 − x)KNNBNTLS–xNT ceramics exhibit low dielectric loss, which is lower than 0.05 and almost keeps constant through a wide temperature range from 25 to 200 °C.

Fig. 5(a) shows the polarization versus electric field (P–E) hysteresis loops of the (1 − x)KNNBNTLS–xNT (x = 0, 0.04, 0.06, 0.1) ceramics at room temperature. Typical hysteresis loops were observed for all the samples. The variations of remanent polarization (P_r) and coercive field (E_c) as a function of x are summarized in Fig. 5(b). It can be seen that P_r decreases initially and then increases slightly with increasing x, while E_c firstly increases rapidly and then decreases as x increases. The value of P_r reaches 17.3 μC/cm^2 at x = 0.06, where the value of E_c is 16.1 kV/cm. These characteristics suggest that the

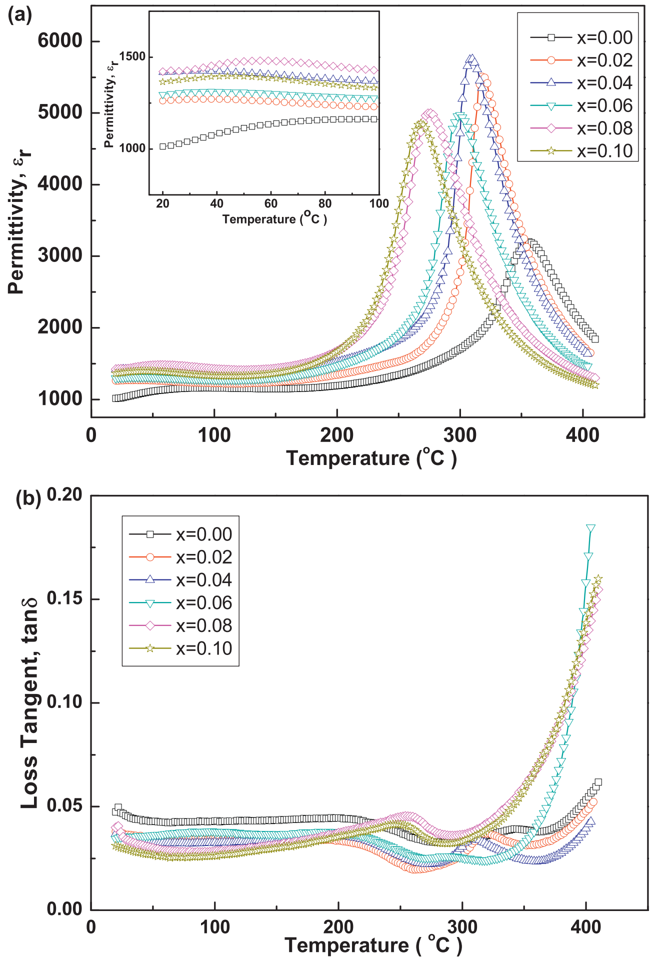

Fig. 4. Temperature dependence of (a) permittivity and (b) loss tangent of the (1 − x)KNNBNTLS–xNT ceramics with different $NaTaO_3$ contents at 10 kHz.

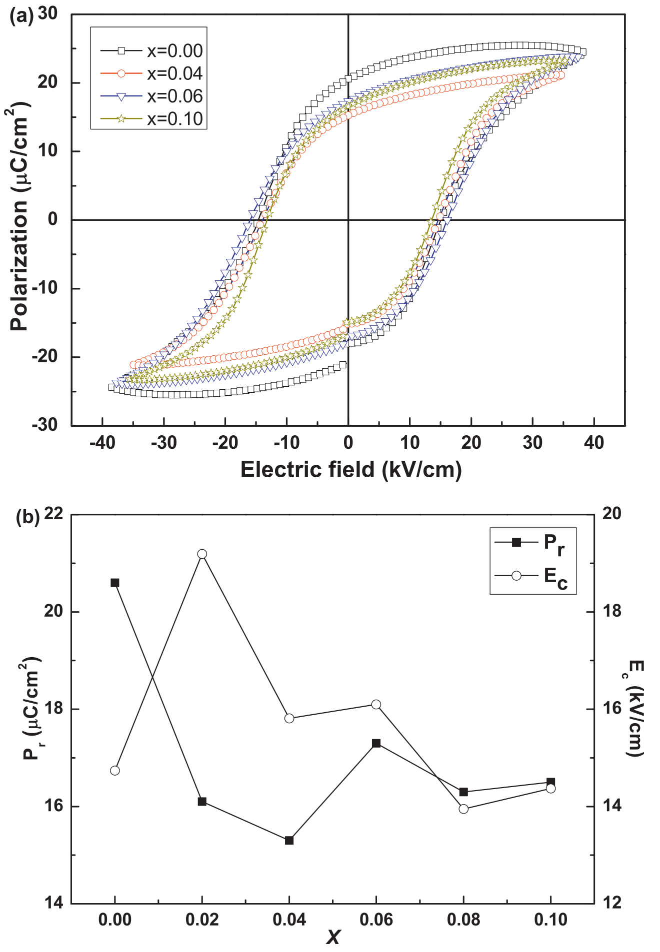

Fig. 5. (a) Polarization hysteresis loops the (1 − x)KNNBNTLS–xNT ceramics at room temperature. (b) The variations of remanent polarization (P_r) and coercive field (E_c) of the ceramics as a function of x.

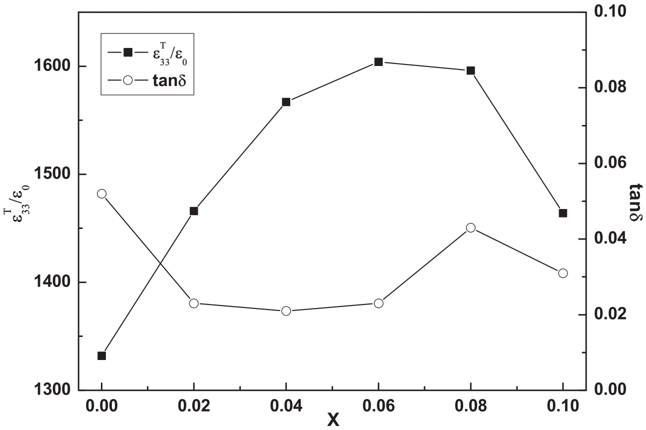

Fig. 6. The relative permittivity, $\varepsilon^T_{33}/\varepsilon_0$, and the dissipation factor, tan δ, of the poled $(1-x)$KNNBNTLS–xNT ceramics as a function of x.

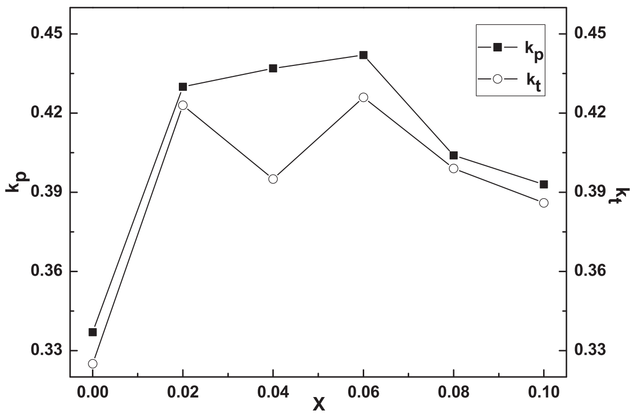

Fig. 8. Electromechanical coupling factors, k_p and k_t, of the $(1-x)$KNNBNTLS–xNT ceramics as a function of x.

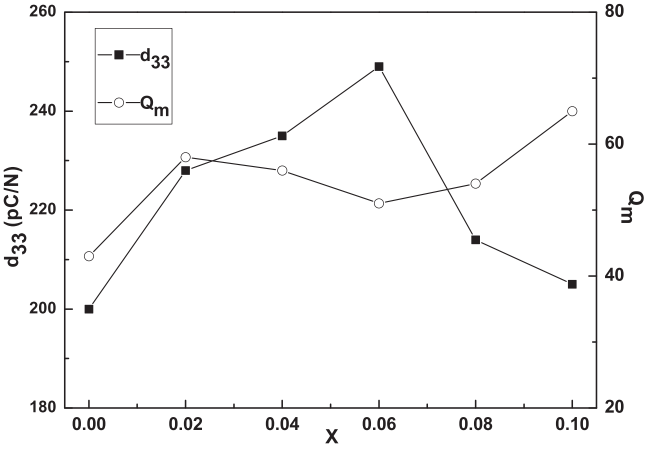

Fig. 7. Piezoelectric constant, d_{33}, and the mechanical quality factor, Q_m, of the $(1-x)$KNNBNTLS–xNT ceramics as a function of x.

addition of $NaTaO_3$ weakens the ferroelectric properties of the $(1-x)$KNNBNTLS–xNT ceramics. It is known that the reduction of the polarization is related to the decrease in tetragonality [30]. Similar phenomena have also been observed in the MnO_2 and $CaTiO_3$ modified (K,Na)NbO_3-based ceramics [31,32]. Therefore, it is attributed to the decrease in tetragonality of the $(1-x)$KNNBNTLS–xNT ceramics that the ferroelectric properties of the ceramics decline with increasing $NaTaO_3$.

Fig. 6 shows the tendency of the relative permittivity, $\varepsilon^T_{33}/\varepsilon_0$, and the dissipation factor, tan δ, of the poled $(1-x)$KNNBNTLS–xNT ceramics as a function of x. It is found that the $\varepsilon^T_{33}/\varepsilon_0$ of the ceramics increases obviously from 1332 to 1604 as x increases from 0 to 0.06. On the contrary, the tan δ decreases rapidly from 0.052 to 0.023 as x increases from 0 to 0.02 and then remains almost unchanged at $0.02 \leq x \leq 0.06$. These results indicate that the dielectric properties of the $(1-x)$KNNBNTLS–xNT ceramics are improved significantly by addition of $NaTaO_3$. Some researches have shown that the dielectric properties of (K,Na)NbO_3-based ceramics are related to the density and grain size distribution [29,33,34]. Therefore, the improvement of the dielectric properties of the $(1-x)$KNNBNTLS–xNT ceramics may be partly attributed to the increase of bulk density of the ceramics induced by addition of $NaTaO_3$. The improvement may also be attributed to partial substitution of Ta^{5+} for Nb^{5+} and Sb^{5+}. Compared with Nb^{5+} and Sb^{5+}, Ta^{5+} possesses a higher polarizability [35]. As a result, Ta^{5+} makes more contribution to the polarity of the ceramics than Nb^{5+} and Sb^{5+}. In addition, a homogeneous grain size distribution induced by addition of $NaTaO_3$ has also made a contribution to the enhancement of dielectric constant.

Fig. 7 shows the piezoelectric constant, d_{33}, and the mechanical quality factor, Q_m, of the $(1-x)$KNNBNTLS–xNT ceramics as a function of x. It can be seen that the d_{33} enhances with increasing x when $x \leq 0.06$ and then decreases rapidly. The maximum d_{33} value of 249 pC/N is obtained at $x = 0.06$. The ceramics have relatively low Q_m value in the range of 43–65, which increases in general as x increases. It is well known that the mechanical quality factor Q_m characterizes the internal friction in a grain induced by the rotation of the spontaneous polarization vector or mobility of domain wall. The degraded ferroelectric properties of the ceramics imply that the amount of spontaneous polarization in the unit volume decreases, and hence the internal friction decreases [36,37]. As a result, Q_m increases with the decrease of the ferroelectric properties. Moreover, Fig. 8 shows the electromechanical coupling factors, k_p and k_t, of the $(1-x)$KNNBNTLS–xNT ceramics as a function of x. The k_p and k_t increase initially and then decrease with increasing x. The maximum values of k_p and k_t, 0.442 and 0.426, are obtained when $x = 0.06$.

All these results indicate that the piezoelectric properties of the $(1-x)$KNNBNTLS–xNT ceramics are enhanced significantly by addition of $NaTaO_3$. For the piezoelectric materials with a tetragonal symmetry, the piezoelectric constant d_{33} values are proportional to the relative permittivity ε_{33} and remnant polarization P_r according to $d_{33} = 2Q_{11}\varepsilon_0\varepsilon_{33}P_3$, where Q_{11} is the electrostrictive coefficient and should not change significantly by doping, ε_{33} is the relative permittivity, and P_3 is the polarization along the polar axis and approximately equals P_r [20]. In this work, it is found that the P_r of the ceramics decreases with the increase of NT content, as shown in Fig. 5.

However, the $\varepsilon_{33}^T/\varepsilon_0$ and the d_{33} of the ceramics show continuous increase when $x \leq 0.06$. Therefore, the enhancement of d_{33} may be attributed to the increase in $\varepsilon_{33}^T/\varepsilon_0$. This is consistent with the result reported by Lin and Kwok [13].

4. Conclusions

The influences of the $NaTaO_3$ on the structure, bulk density, dielectric, ferroelectric and piezoelectric properties of the $(1-x)$KNNBNTLS–xNT ceramics have been studied. The ceramics sintered in air at 1060–1140 °C for 3–4 h formed single phase perovskite solid solutions with the tetragonal symmetry. The bulk density of the ceramics was improved by addition of $NaTaO_3$. The orthorhombic–tetragonal transition temperature $T_{\mathrm{O-T}}$ of the ceramics shifted to below room temperature with the addition of $NaTaO_3$. The dielectric and piezoelectric properties of ceramics were enhanced by addition of $NaTaO_3$. The outstanding electrical properties of $d_{33} = 249$ pC/N, $Q_m = 51$, $k_p = 0.442$, $k_t = 0.426$, $P_r = 17.3\ \mu C/cm^2$, $E_c = 16.1$ kV/cm, $\varepsilon_{33}^T/\varepsilon_0 = 1604$ and $\tan\delta = 0.023$ were obtained at $x = 0.06$.

Acknowledgements

This work was supported by the Research and Innovation Foundation of China University of Geosciences, China. The authors are grateful to Mr. Jishun Yu for XRD analysis and Ms. Huawei Tang for assistance in performing the dielectric and piezoelectric property measurements.

References

[1] M. Kosec, B. Malič, A. Benčan, T. Rojac, KNN-based piezoelectric ceramics, in: A. Safari, E.K. Akdoğan (Eds.), Piezoelectric and Acoustic Materials for Transducer Applications, Springer, New York, 2008, pp. 81–102.
[2] L. Egerton, D.M. Dillom, Piezoelectric and dielectric properties of ceramics in the system potassium–sodium niobate, J. Am. Ceram. Soc. 42 (1959) 438–442.
[3] Y. Saito, H. Takao, T. Tani, T. Nonoyama, K. Takatori, T. Homma, T. Nagaya, M. Nakamura, Lead-free piezoceramics, Nature 432 (2004) 84–87.
[4] K. Wang, J.F. Li, Domain engineering of lead-free Li-modified (K,Na)NbO_3 polycrystals with highly enhanced piezoelectricity, Adv. Funct. Mater. 20 (2010) 1924–1929.
[5] Y.P. Guo, K.I. Kakimoto, H. Ohsato, $(Na_{0.5}K_{0.5})NbO_3$–$LiTaO_3$ lead-free piezoelectric ceramics, Mater. Lett. 59 (2005) 241–244.
[6] Y.P. Guo, K.I. Kakimoto, H. Ohsato, Phase transitional behavior and piezoelectric properties of $(Na_{0.5}K_{0.5})NbO_3$–$LiNbO_3$ ceramics, Appl. Phys. Lett. 85 (2004) 4121–4123.
[7] G.Z. Zang, J.F. Wang, H.C. Chen, W.B. Su, C.M. Wang, P. Qi, B.Q. Ming, J. Du, L.M. Zheng, S.J. Zhang, T.R. Shrout, Perovskite $(Na_{0.5}K_{0.5})_{1-x}(LiSb)_xNb_{1-x}O_3$ lead-free piezoceramics, Appl. Phys. Lett. 88 (2006) 212908–212910.
[8] Y.P. Guo, K.I. Kakimoto, H. Ohsato, Dielectric and piezoelectric properties of lead-free $(Na_{0.5}K_{0.5})NbO_3$–$SrTiO_3$ ceramics, Solid State Commun. 129 (2004) 279–284.
[9] R.Z. Zuo, X.S. Fang, C. Ye, Phase structures and electrical properties of new lead-free $(Na_{0.5}K_{0.5})NbO_3$–$(Bi_{0.5}Na_{0.5})TiO_3$ ceramics, Appl. Phys. Lett. 90 (2007) 092904–092906.
[10] H.Y. Park, K.H. Cho, D.S. Paik, S. Nahm, H.G. Lee, D.H. Kim, Microstructure and piezoelectric properties of lead-free $(1-x)(Na_{0.5}K_{0.5})NbO_3$–$x$$CaTiO_3$ ceramics, Appl. Phys. Lett. 102 (2007) 124101–124105.
[11] H.L. Du, W.C. Zhou, F. Luo, D.M. Zhu, S.B. Qu, Y. Li, Z.B. Pei, Design and electrical properties' investigation of $(K_{0.5}Na_{0.5})NbO_3$–$BiMeO_3$ lead-free piezoelectric ceramics, J. Appl. Phys. 104 (2008) 034104–034107.
[12] M.H. Jiang, X.Y. Liu, G.H. Chen, Phase structures and electrical properties of new lead-free $Na_{0.5}K_{0.5}NbO_3$–$LiSbO_3$–$BiFeO_3$ ceramics, Scripta Mater. 60 (2009) 909–912.
[13] D.M. Lin, K.W. Kwok, Piezoelectric properties of $K_{0.47}7Na_{0.47}Li_{0.06}NbO_3$–$NaSbO_3$ lead-free ceramics for ultrasonic transducer applications, Int. J. Appl. Ceram. Technol., in press, doi:10.1111/j.1744-7402.2010.02500.x.
[14] J. Fu, R.Z. Zuo, X.H. Wang, L.T. Li, Phase transition characteristics and piezoelectric properties of compositionally optimized alkaline niobate based ceramics, J. Alloys Compd. 486 (2009) 790–794.
[15] L. Wu, D.Q. Xiao, X. Li, J.G. Zhu, P. Yu, Y. Sun, Y.Y. Wang, Temperature stability of electrical properties of $(K_{0.5}Na_{0.5})_{1-x}Li_xNb_{0.95}Sb_{0.05}O_3$ lead-free ceramics, Int. J. Appl. Ceram. Technol. 7 (2010) E39–E45.
[16] S.J. Zhang, R. Xia, T.R. Shrout, Modified $(K_{0.5}Na_{0.5})NbO_3$ based lead-free piezoelectrics with broad temperature usage range, Appl. Phys. Lett. 91 (2007) 132913–132915.
[17] S.J. Zhang, R. Xia, H. Hao, H.X. Liu, T.R. Shrout, Mitigation of thermal and fatigue behavior in $K_{0.5}Na_{0.5}NbO_3$-based lead free piezoceramics, Appl. Phys. Lett. 92 (2008) 152904–152906.
[18] J.G. Wu, D.Q. Xiao, Y.Y. Wang, W.J. Wu, B. Zhang, J. Li, J.G. Zhu, $CaTiO_3$-modified $[(K_{0.5}Na_{0.5})_{0.94}Li_{0.06}](Nb_{0.94}Sb_{0.06})O_3$ lead-free piezoelectric ceramics with improved temperature stability, Scripta Mater. 59 (2008) 750–752.
[19] T.A. Skidmore, T.P. Comyn, S.J. Milne, Temperature stability of $([Na_{0.5}K_{0.5}NbO_3]_{0.93}$–$[LiTaO_3]_{0.07})$ lead-free piezoelectric ceramics, Appl. Phys. Lett. 94 (2009) 222902–222904.
[20] A.L. Kholkin, N.A. Pertsev, A.V. Goltsev, Piezoelectricity and crystal symmetry, in: A. Safari, E.K. Akdoğan (Eds.), Piezoelectric and Acoustic Materials for Transducer Applications, Springer, New York, 2008, pp. 17–38.
[21] Y.X. Liu, Y.Q. Huang, H.W. Du, H.L. Li, G.X. Zhang, Crystal structure and properties of $K_{0.5}Na_{0.5}NbO_3$–$Bi_{0.5}Na_{0.5}TiO_3$–$LiSbO_3$ lead-free piezoelectric ceramics, J. Alloys Compd. 506 (2010) 407–411.
[22] R.H. Michel, R.P. Liferovich, A structural study of the perovskite series $Ca_{1-x}Na_xTi_{1-x}Ta_xO_3$, J. Solid State Chem. 177 (2004) 4420–4427.
[23] X.M. Chen, Y.T. Lu, D.Z. Jin, X.Q. Liu, Dielectric and ferroelectric characterization of Na(Ta,Nb)O_3 solid solution ceramics, J. Electroceram. 15 (2005) 21–26.
[24] J. König, B. Jančar, D. Suvorov, New $Na_{0.5}Bi_{0.5}TiO_3$–$NaTaO_3$-based perovskite ceramics, J. Am. Ceram. Soc. 90 (2007) 3621–3627.
[25] R.D. Shannon, Revised effective ionic radii and systematic studies of interatomic distances in halides and chalcogenides, Acta Cryst. A32 (1976) 751–767.
[26] Y. Zhou, M. Guo, C. Zhang, M. Zhang, Hydrothermal synthesis and piezoelectric property of Ta-doping $K_{0.5}Na_{0.5}NbO_3$ lead-free piezoelectric ceramic, Ceram. Int. 35 (2009) 3253–3258.
[27] J. Fu, R.Z. Zuo, X.S. Fang, K. Liu, Lead-free ceramics based on alkaline niobate tantalate antimonate with excellent dielectric and piezoelectric properties, Mater. Res. Bull. 44 (2009) 1188–1190.
[28] P. Zhao, B.P. Zhang, J.F. Li, High piezoelectric d_{33} coefficient in Li-modified lead-free (Na,K)NbO_3 ceramics sintered at optimal temperature, Appl. Phys. Lett. 90 (2007) 242909–242911.
[29] S.J. Liu, B. Wan, P. Wang, S.H. Song, Influence of A-site non-stoichiometry on structure and electrical properties of $K_{0.5}Na_{0.5}NbO_3$-based lead-free piezoelectric ceramics, Scripta Mater. 63 (2010) 124–127.
[30] C. Lichtensteiger, J.M. Triscone, J. Junquera, P. Ghosez, Ferroelectricity and tetragonality in ultrathin $PbTiO_3$ films, Phys. Rev. Lett. 94 (2005) 047603–047606.
[31] J.G. Wu, D.Q. Xiao, Y.Y. Wang, J.G. Zhu, W. Shi, W.J. Wu, B. Zhang, J. Li, Phase structure, microstructure and ferroelectric properties of $(1-x)[(K_{0.50}Na_{0.50})_{0.94}Li_{0.06}](Nb_{0.94}Sb_{0.06})O_3$–$x$$CaTiO_3$ lead-free ceramics, J. Alloys Compd. 476 (2009) 782–786.

[32] D.M. Lin, K.W. Kwok, H.L.W. Chan, Effects of MnO_2 on the microstructure and electrical properties of $0.94(K_{0.5}Na_{0.5})NbO_3$–$0.06Ba(Zr_{0.05}Ti_{0.95})O_3$ lead-free ceramics, Mater. Chem. Phys. 109 (2008) 455–458.

[33] E. Atamanik, V. Thangadurai, Dielectric properties of Ga-doped $Na_{0.5}K_{0.5}NbO_3$, J. Phys. Chem. C 113 (2009) 4648–4653.

[34] E.M. Alkoy, M. Papila, Microstructural features and electrical properties of copper oxide added potassium sodium niobate ceramics, Ceram. Int. 36 (2010) 1921–1927.

[35] J. Rodel, W. Jo, K.T.P. Seifert, E.M. Anton, T. Granzow, D. Damjanovic, Perspective on the development of lead-free piezoceramics, J. Am. Ceram. Soc. 92 (2009) 1153–1177.

[36] L. Wu, C.C. Wei, T.S. Wu, H.C. Liu, Piezoelectric properties of modified PZT ceramics, J. Phys. C: Solid State Phys. 16 (1983) 2813–2821.

[37] Q. Chen, Z.H. Peng, H. Liu, D.Q. Xiao, J.L. Zhu, J.G. Zhu, The crystalline structure and phase-transitional behavior of $(Li_{0.12}Na_{0.88})(Nb_{1-x\%}Sb_{x\%})O_3$ lead-free piezoelectric ceramics with high Q_m, J. Am. Ceram. Soc. 93 (2010) 2788–2794.